J. Chil. Chem. Soc., 63, Nº 1 (2018)

THEORETICAL STUDY ON THE HYDROGEN BONDING INTERACTIONS IN PARACETAMOL-WATER COMPLEXES

*MEIFANG XU[a,b], BOHAI ZHANG[a], QI WANG[a], YUAN YUAN[a], LE SUN[a], ZHENGGUO HUANG[a1]**

[a] *Tianjin Key Laboratory of Structure and Performance for Functional Molecules; Key Laboratory of Inorganic-Organic Hybrid Functional Materials Chemistry (Tianjin Normal University), Ministry of Education; College of Chemistry, Tianjin Normal University, Tianjin 300387, People's Republic of China*
[b] *College of Mathematics Science, Tianjin Normal University, Tianjin 300387, People's Republic of China*

ABSTRACT

The paracetamol–water (PA–H_2O) complexes formed by hydrogen bonding interactions were investigated at the MP2/6–311++G(d,p) level. Six PA–H_2O complexes possessing various types of hydrogen bonds (H–bonds) were characterized by geometries, energies, vibrational frequencies. Natural bond orbital (NBO), quantum theory of atoms in molecules (QTAIM) and the localized molecular orbital energy decomposition analysis (LMO–EDA) were performed to explore the nature of the hydrogen–bonding interactions in these complexes. The intramolecular H–bond formed between the methylene and carbonyl oxygen atom of paracetamol is retained in most of complexes. The H–bonds in PW1 and PW6 are stronger than other H–bonds, moreover, the researches show that both the hydrogen bonding interaction and structural deformation play important roles for the relative stabilities of PA–H_2O complexes.

Keyword: paracetamol; hydrogen bonding interactions; natural bond orbital (NBO); quantum theory of atoms in molecules (QTAIM)

1. INTRODUCTION

Paracetamol (PA) is a widely used non-prescription drug, which can enhances the analgetic activity and reduces the nephrotoxicity [1]. A randomized controlled trial of chronic pain from osteoarthritis in adults found similar benefit from PA and diclofenac . In recommended doses, the side effects of PA are mild to non–existent, but acute overdoses of PA can cause potentially fatal kidney, brain and liver damage and, in rare individuals, a normal dose can do the same [2-6]. The risk may be heightened by chronic alcohol abuse. PA toxicity is the foremost cause of acute liver failure and accounts for most drug overdoses [7-12].

The infrared and Raman spectra of PA have been studied widely [13-17]. Joseph M. et al. have measured the resonant 2–photon ionization spectrum of jet–cooled PA, and analyzed the results in the light of theoretical calculations of the ground–state geometry and vibrational frequencies [18]. The complexes formed by PA with ethanol and acetone species have been studied by Y. Danten et al. [19]. Two nearly isoenergetic conformers were distinctly found in a supersonic molecular beam expansion and positively identified as the cis– and trans– isomers of PA by UV–UV hole–burning spectroscopy [20].

Weak interactions, especially hydrogen bonding interaction, play important roles in biological systems [21-26]. For example, hydrogen bonding interaction construct the structure of DNA and RNA (bonding between nitrogenous bases), the secondary structure of proteins (helix or pleated sheet) and the different branching patterns of sugar chains. For the pharmacological activity of PA, it is of importance to have information about the conformation of PA in solution, and hydrogen bonding interaction plays an important role on the conformations of PA since it is the major interaction in solution of PA. However, there is few literatures can be found so far. Therefore, we dedicated to study the hydrogen bonding interaction between PA and H_2O solvent molecule by ab initio method, and we hope that this study will be helpful to the further study on the solvent effects of PA. It is important to note that not all theoretical methods are reliable for the description of hydrogen bond (H–bond) because it is usually weak. Compared with density functional theory (DFT), MP2 is too time-consuming to apply to large biomolecular systems even with a medium-size basis set, however, it is a reliable method to descript H–bond because it treats electron correlation well. Therefore, here MP2 was used to study the hydrogen bonding interactions in PA–H_2O complexes. The geometric parameters (bond length and bond angle) of H–bond usually provide us preliminary information about the strength of H–bond. However, more technical tools are required to elucidate the nature of H–bond in PA–H_2O complexes. The quantum theory of atoms in molecules (QTAIM) [27, 28], natural bond orbital (NBO) analysis [29] and the localized molecular orbital energy decomposition analysis (LMO–EDA) [30] methods meet this requirements since they have been proved to be very useful tools in understanding of H–bond [31-36]. Therefore, ab initio calculations combined with QTAIM, NBO and LMO-EDA approaches were performed to investigate the hydrogen bonding interactions in PA–H_2O complexes.

2. COMPUTATIONAL DETAILS

The PA and water monomers were optimized at MP2/6–311++G (d,p) level , then the PA–H_2O complexes were constructed starting from the most stable monomers and were fully optimized at the same level. Harmonic vibrational frequencies calculations were carried out to characterize the structures as minima and enable the evaluation of zero–point vibrational energies (ZPVE). To take into account the effects of the basis set superposition error (BSSE), the counterpoise corrections were implemented to insure that complexes and monomers are being computed with a consistent basis set. Then the interaction energies were calculated based on the ZPVE and BSSE corrections.

In order to analyze the properties of the H–bonds in complexes, QTAIM, NBO and LMO-EDA calculations were carried out. According to QTAIM, the first descriptor of X–H···Y H–bond is the existence of the bond critical point (BCP) at the H···Y bond. Moreover, some descriptors at BCPs have been used widely to characterize the bonding between the atoms, such as the electron density (ρ_b), the Laplacian of electron density ($\nabla^2\rho_b$) and the total energy density (H_b) [37]. Both ρ_b and $\nabla^2\rho_b$ at the H···Y BCP are good measures of the strength of H–bond. According to the criteria established by Koch and Popelier [38], the $\nabla^2\rho_b$ should fall in the range of 0.024–0.139 a.u., and the ρ_b is within 0.002–0.034 a.u.. Such criteria can used to distinguish hydrogen–bonding interactions from van der Waals interactions. The total electron energy density (H_b) is the sum of the potential energy density (V_b) and kinetic energy density (G_b), which can also be used to characterize the interactions between atoms. The local priority of V_b at the BCP results into a negative H_b, which means a partial covalent character is attributed to the H–bonds. Meanwhile, the low and positive $\nabla^2\rho_b$ at the BCP means typical closed–shell interactions. Therefore, both H_b and $\nabla^2\rho_b$ at the BCP can used to characterize the interaction [39-42]: for very strong H–bonds, $\nabla^2\rho_b$ <0 and H_b <0; for weak or medium–strength H–bonds, $\nabla^2\rho_b$ >0 and H_b >0; for strong H–bonds, $\nabla^2\rho_b$ >0 and H_b <0.

According to NBO theory [43], the formation of H–bond results into that electron density from the lone pair n_B of the H–acceptor delocalizes into the unfilled σ^*_{XH} anti–bonding orbital of the H–donor. Therefore, the occupancy of the σ^*_{XH} anti–bond orbital increases, which leads to that the X–H bond is weakened and lengthened. The charge transfer (CT) effects between n_B and σ^*_{XH} is estimated by second–order perturbation energies $E(2)$, in other words, the $E(2)$ lowering is responsible for the orbital interaction of H–bond, the larger $E(2)$ values correspond to stronger CT interaction occurred in the H–bond. In LMO–EDA, total interaction energy ΔE_{MP2} is decomposed into five terms: electrostatic energy (ΔE_{ele}), exchange energy (ΔE_{ex}), repulsion energy (ΔE_{rep}), polarization energy (ΔE_{pol}) and dispersion energy (ΔE_{disp}). The ab initio and NBO calculations were carried out using Gaussian 09 [44], QTAIM analysis was performed using the wave functions obtained at the MP2/6–311++G(d,p) level by AIM2000 [45], and the LMO–EDA was implement at the same level using the Gamess program [46].

e-mail: hsxyhzg@126.com

3. RESULTS AND DISCUSSION

The PA and water monomers were optimized at the MP2/6–311++G(d,p) level, and the molecular graphs are presented in Figure 1. As shown in Figure 1, water molecule can donate/accept proton to form H–bond, in which the hydroxyl and oxygen atom act as H–donor/acceptor, respectively. PA has several possible proton–donor/acceptor sites to form H–bonds. The imino group in the benzene ring and the phenolic hydroxyl are the main H–donor sites of PA, while the methylene can also form weak H–bonds with water in some complexes. The main H–acceptors of PA are the oxygen atoms of the hydroxyl and carbonyl groups. Moreover, the oxygen atom of the carbonyl groups usually accepts one proton to form intramolecular H–bond with the methylene.

3.1 Structures

All molecular graphs of optimized PA–H_2O complexes are shown in Figure 2, and the structural parameters of H–bonds are listed in Table 1. As shown in Figure 2, different types of

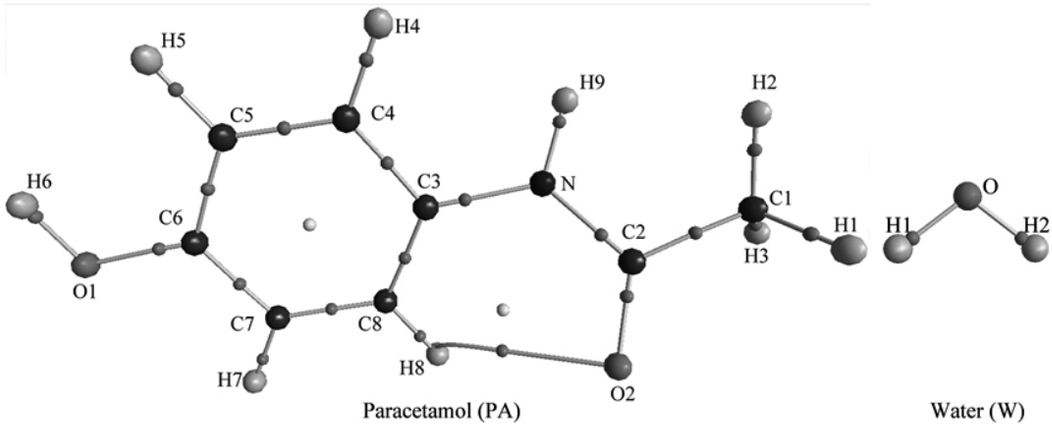

Figure 1. Molecular graphs of paracetamol (PA) and water (W) monomers. Large circles correspond to attractors attributed to atomic positions: white, H; blue, N; gray, C; red, O. Small circles are attributed to critical points: red, bond critical point; yellow, ring critical point.

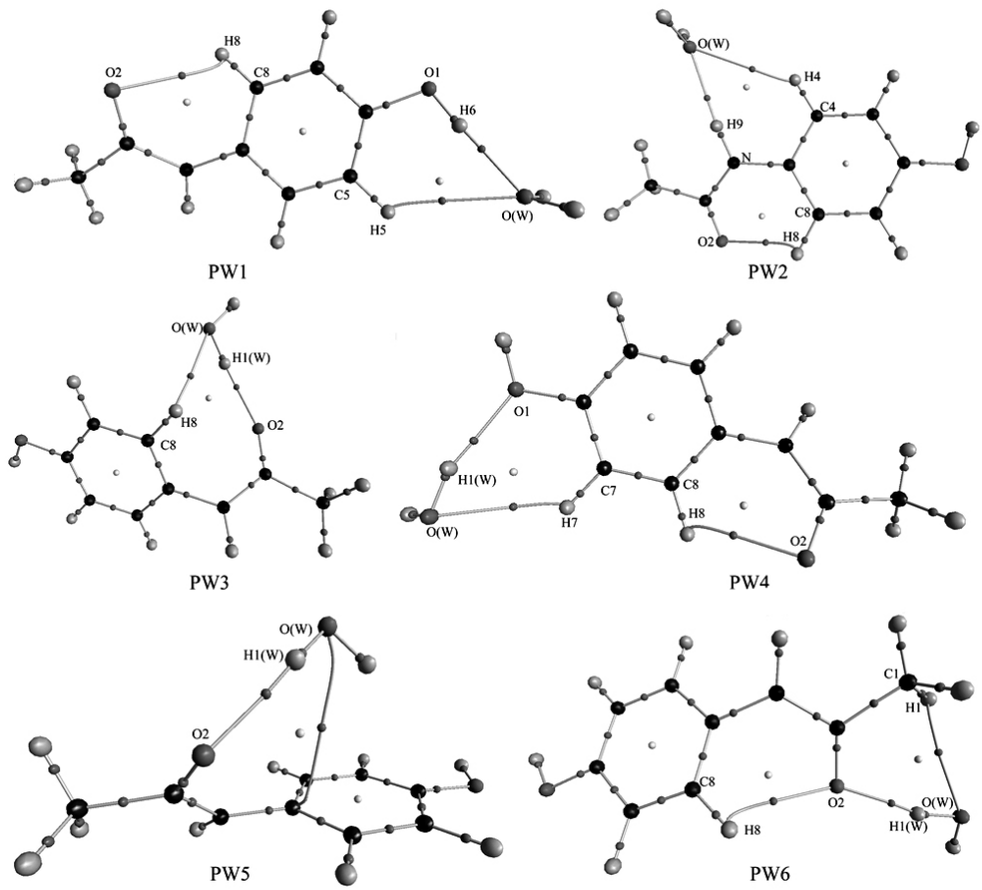

Figure 2. Molecular graphs of PA–H_2O complexes. Large circles correspond to attractors attributed to atomic positions: white, H; blue, N; gray, C; red, O. Small circles are attributed to critical points: red, bond critical point; yellow, ring critical point.

Table 1. Structural parameters (bond lengths in Å, angles in degrees) of H–bonds in PA–H_2O complexes calculated at the MP2/6–311++G(d,p) level.

complex	H–bond[a]	$R_{X–H}$	$\Delta R_{X–H}$[b]	$R_{H\cdots Y}$	$\delta R_{H\cdots Y}$	$\theta_{X–H\cdots Y}$
PW1	$C8H8^{PA}\cdots O2^{PA}$	1.083	0.001	2.392	0.328	109.4
	$C5H5^{PA}\cdots O^{W}$	1.087	-0.001	2.681	0.039	128.4
	$O1H6^{PA}\cdots O^{W}$	0.970	0.008	1.878	0.842	177.5
PW2	$C8H8^{PA}\cdots O2^{PA}$	1.082	-0.001	2.269	0.451	115.2
	$C4H4^{PA}\cdots O^{W}$	1.087	-0.001	2.695	0.025	135.7
	$NH9^{PA}\cdots O^{W}$	1.014	0.005	2.032	0.688	173.9
PW3	$C8H8^{PA}\cdots O^{W}$	1.084	0.002	2.479	0.241	120.3
	$OH1^{W}\cdots O2^{PA}$	0.968	0.008	1.930	0.790	166.1
PW4	$C8H8^{PA}\cdots O2^{PA}$	1.082	0.000	2.347	0.373	111.0
	$C7H7^{PA}\cdots O^{W}$	1.086	0.000	2.537	0.183	135.4
	$OH1^{W}\cdots O1^{PA}$	0.965	0.005	1.985	0.735	162.0
PW5	$OH1^{W}\cdots O2^{PA}$	0.967	0.007	2.017	0.703	168.8
PW6	$C8H8^{PA}\cdots O2^{PA}$	1.083	0.001	2.417	0.303	107.0
	$OH1^{W}\cdots O2^{PA}$	0.970	0.011	1.885	0.835	165.1
	$C1H1^{PA}\cdots O^{W}$	1.091	-0.002	2.624	0.096	117.0
PA	C8H8	1.082		2.367	0.353	110.1
	C5H5	1.088				
	O1H6	0.962				
	C4H4	1.088				
	NH9	1.010				
	C7H7	1.086				
	C1H1	1.093				
Water	OH	0.960				

[a] Superscript "PA" denotes paracetamol and superscript "W" denotes H_2O
[b] $\Delta R_{X–H}=R_{X–H}$ (complexes) − $R_{X–H}$(free monomer)

H–bonds are formed in PA–H_2O complexes. According to QTAIM, the H–bond, including inter– or intramolecular H–bonds, is characterized by the BCPs between H–donor (X–H) and H–acceptor (Y), and ring structure formed by multiple H–bonds is characterized by a ring critical point (RCP). The shorter distance between the RCP and corresponding BCP means less stability of the H–bond [47-50]. As a note, the RCP at the center of the ring of benzene has nothing to do with H–bond. As shown in Figs. 1 and 2, one intramolecular $C8H8^{PA}\cdots O2^{PA}$ H–bond formed between the methylene and the oxygen atom can be found in PA monomer, which is retained in all PA–H_2O complexes except PW3 and PW5.

As shown in Fig. 2, PW3 have two H–bonds, but PW5 have one H–bond. The $C8H8^{PA}\cdots O2^{PA}$ intramolecular H–bond in PW3 is replaced by two intermolecular H–bonds, in which water monomer acts as H–donor and H–acceptor simultaneously. Similarly, the $C8H8^{PA}\cdots O2^{PA}$ intramolecular H–bond in PW5 is also replaced by one intermolecular H–bond formed between the hydroxyl of water moiety donating one proton to oxygen atom of the carbonyl groups in PA moiety. Therefore, it can learn that the serious structural deformations occurred in PW3 and PW5. In addition, it worth noting that there seems to be one π H–bond formed between the hydroxyl of water and the benzene ring of PA monomer, and the distance between the hydrogen atom and the center of the benzene ring is 2.738 Å. Unfortunately, such π H–bond cannot be characterized by QTAIM directly. Except for the $C8H8^{PA}\cdots O2^{PA}$ intramolecular H–bond, other complexes have two intermolecular H–bonds. The oxygen atom of water moiety accepts two protons from the hydroxyl and methylene of PA simultaneously to form one bifurcated H–bond in PW1. Another bifurcated H–bond can be found in PW2, which is formed by the oxygen atom of water moiety accepts two protons from the hydroxyl and imino of PA simultaneously. For the PW4 and PW6 complexes, two intermolecular H–bonds are formed, in which water monomer acts as H–donor and H–acceptor, respectively.

The change ($\Delta R_{X–H}$) of the X–H bond with respect to the corresponding X–H bond in free monomers (PA or water) reflects the nature of H–bond, the elongation of the X–H bond corresponds to red–shifting H–bond, while the shortening of the X–H bond represents blue–shifting one. In addition, the distance of the H···Y bond reflects the strength of the hydrogen bonding interaction as well. As shown in Table 1, for most of the complexes, the $\Delta R_{X–H}$ of the H–bonds taking methylene as H–donors are negative or remain little changes, which indicates that they are very weak H–bonds. All other H–bonds have positive $\Delta R_{X–H}$ values and are red–shifting ones. The largest $\Delta R_{X–H}$ (0.011 Å) is found in the $OH1^{W}\cdots O2^{PA}$ H–bond of PW6, which indicates that it is the strongest intermolecular H–bond. It is worth noting that another intermolecular H–bond ($O1H6^{PA}\cdots O^{W}$) in PW1 is also strong, considering its short $R_{H\cdots Y}$ (1.878 Å). However, its $\Delta R_{X–H}$ (0.008 Å) is smaller than that of the $OH1^{W}\cdots O2^{PA}$ H–bond in PW6. Therefore, for such case, $\Delta R_{X–H}$ is not the unique technical means to estimate the strength of the H–bond, while $R_{H\cdots Y}$ is an alternative choice. As shown in Table 1, the shortest of $R_{H\cdots Y}$ is 1.878 Å of the intermolecular $O1H6^{PA}\cdots O^{W}$ H–bond in PW1, which seems to be the strongest H–bond. Of course, another intermolecular H–bond in PW6, $OH1^{W}\cdots O2^{PA}$, is also strong H–bonds due to its shorter $R_{H\cdots Y}$ (1.885 Å). For the H–bonds in which methylene acts as H–donor in some PA complexes (PW1, PW2, PW4 and PW6), the $R_{H\cdots Y}$ values are small and close to the sum of the van der Waals radii of the H and Y atoms. Therefore, from a structural viewpoint, the interaction between the methylene and Y atom is very weak and has partial van der Waals character.

3.2 Vibrational Frequencies

The harmonic vibrational frequencies of H–bonds in PA–H_2O complexes and monomers as well as their shifts calculated at the MP2/6–311++G(d,p) level are listed in Table 2. The shift ($\Delta\nu_{X–H}$) of the X–H stretching vibrational frequency is one of the main fingerprints of H–bonds. It is generally accepted that the X–H bond is weakened due to the formation of an H–bond, which lead to the red shift of $\nu_{X–H}$. The larger the $\Delta\nu_{X–H}$ is, the stronger the H–bond is. However, it is

Table 2. The X–H stretching vibrational frequencies (strength) of H–bonds in both PA–H_2O complexes and monomers.

complex	H–bond	ν_{X-H} [a]	$\Delta\nu_{X-H}$
PW1	$C8H8^{PA}\cdots O2^{PA}$	3263.2(0,s)[b]	-4.2
	$C5H5^{PA}\cdots O^{W}$	3218.5(2,s)[c]	13.4
	$O1H6^{PA}\cdots O^{W}$	3724.8(684)[d]	-151.2
PW2	$C8H8^{PA}\cdots O2^{PA}$	3273.7(3,s)[b]	6.3
	$C4H4^{PA}\cdots O^{W}$	3215.2(2,s)[e]	10.1
	$NH9^{PA}\cdots O^{W}$	3588.2(237)[d]	-71
PW3	$C8H8^{PA}\cdots O^{W}$	3254.6(2,s)[b]	-12.8
	$OH1^{W}\cdots O2^{PA}$	3962.6(107,as),3780.2(272,s)	-40, -104.1
PW4	$C8H8^{PA}\cdots O2^{PA}$	3269.7(2,s)[b]	2.3
	$C7H7^{PA}\cdots O^{W}$	3229.8(4,as)[f]	2.3
	$OH1^{W}\cdots O1^{PA}$	3969.4(138,as),3816.4(194,s)[g]	-33.2, -67.9
PW5	$OH1^{W}\cdots O2^{PA}$	3942.2(46,as),3799.0(169,s)	-60.4, -85.3
PW6	$C8H8^{PA}\cdots O2^{PA}$	3262.7(0,s)[b]	-4.7
	$OH1^{W}\cdots O2^{PA}$	3961.7(108,as),3710.5(580,s)[h]	-40.9, -173.8
	$C1H1^{PA}\cdots O^{W}$	3196.6(3,as)[i],3086.6(7,s)[j]	18.3, 0.4
PA	C8H8	3267.4(1,s)[b]	
	C5H5	3205.1(8,s)[c]	
	O1H6	3876.0(77)	
	C4H4	3205.1(8,s)[b]	
	NH9	3659.2(30)	
	C7H7	3227.5(2,as)[f]	
	C1H1	3178.3(9,as)[i],3086.2(8,s)[j]	
Water	OH	4002.6(63,as),3884.3(13,s)	

[a] All frequencies are in cm^{-1} and the strengths are in $km\cdot mol^{-1}$. "as" denotes the asymmetric stretching vibration mode, and "s" denotes the symmetric stretching vibration mode.
[b] Mixing occurs among the C7H7 and C5H5 stretching vibration modes
[c] Mixing occurs among the C8H8 and C4H4 stretching vibration modes
[d] Mixed with symmetric H–O–H stretching vibration mode of free water molecule slightly.
[e] Mixing occurs among the C5H5 ,C7H7 and C8H8 stretching vibration modes
[f] Mixing occurs among the C8H8 and C4H4 stretching vibration modes
[g] Slight mixing with O1H6 stretching vibration modes
[h] Slight mixing with NH9 stretching vibration modes
[i] Strong mixing with asymmetric H3–C2–H2 stretching vibration modes
[j] Strong mixing with symmetric H3–C2–H2 stretching vibration modes

hard to calculate the $\Delta\nu_{X-H}$ when the X–H stretching vibrational mode mixes with other vibrational modes. For example, the mixture between C1H1 and asymmetric/symmetric H3–C2–H2 stretching vibration modes in free PA molecule are calculated to be 3178.3 and 3086.2 cm^{-1}, respectively, so two $\Delta\nu_{X-H}$ values may be given for such H–bonds involving C1H1 as H–donor. Similar things are also seen for PA–H_2O complexes. Taking PW4 as an example, the symmetric stretching vibrational mode of $OH1^{W}\cdots O1^{PA}$ mixes with O1H6, and the values of $\Delta\nu_{X-H}$ with respect to the corresponding stretching vibration modes in free H_2O molecule are calculated to be -33.2 and -67.9 cm^{-1}, respectively. As shown in Table 2, the largest red–shift value of -173.8 cm^{-1} is found for the $OH1^{W}\cdots O2^{PA}$ H–bond in PW6. The $O1H6^{PA}\cdots O^{W}$ (PW1) and $OH1^{W}\cdots O2^{PA}$ (PW3) H–bonds have large red–shifts of more than -100 cm^{-1}, so the strengths of these H–bonds are regarded as weaker than the $OH1^{W}\cdots O2^{PA}$ H–bonds in PW6 and stronger than other red–shifted H–bonds. Other intermolecular H–bonds in the PA–H_2O complexes are weaker since their absolute values of $\Delta\nu_{X-H}$ are less than 100 cm^{-1}. There are seven blue–shifted H–bonds which have positive shift values of $\Delta\nu_{X-H}$, moreover, they are usually weaker than the red–shifted ones and a partial dispersion character is attributed to them. However, the small $\Delta\nu_{X-H}$ of the intramolecular $C8H8^{PA}\cdots O2^{PA}$ H–bond in PA–H_2O complexes does not mean that it is also very weak, as it originally existed in the free PA molecule.

3.3 Bonding analyses

The electronic topological properties at the H···Y BCPs of H–bonds, including the electron density (ρ_b), the Laplacian of the electron density ($\nabla^2\rho_b$), the kinetic energy density (G_b), the potential energy density (V_b), and the total electron energy density (H_b), for all of the complexes and monomer are listed in Table 3. As shown in Table 3, among all PA–H_2O complexes and PA monomer, both the H_b and $\nabla^2\rho_b$ of all H–bonds are positive and fall in the ranges proposed by Popelier, thus they are considered as weak or medium H–bonds. Especially, for the H–bonds taking methylene as H–donor, both ρ_b and $\nabla^2\rho_b$ are close to the lower limit of criteria proposed by Popelier, which shows that they are very weak and partial dispersion character is attributed to them. Moreover, the H–bonds involving the hydroxyl as H-donors are stronger than other ones due to larger ρ_b and $\nabla^2\rho_b$. Especially, for the $OH1^{W}\cdots O2^{PA}$ (PW6) and $O1H6^{PA}\cdots O^{W}$ (PW1) H–bonds, both ρ_b and $\nabla^2\rho_b$ of them are the largest among all H–bonds, which indicates that they are the two strongest H–bonds.

Table 3. The electron density (ρ_b) and its Laplacian ($\nabla^2\rho_b$), total electron energy density (H_b), potential energy density (V_b) and Lagrangian form of kinetic energy density (G_b) in a.u. at H···Y BCPs of H–bonds in PA–H_2O complexes obtained by QTAIM analysis.

complex	H–bond	ρ_b	$\nabla^2\rho_b$	H_b	V_b	G_b
PW1	$C8H8^{PA}\cdots O2^{PA}$	0.01322	0.05192	0.00174	-0.00951	0.01124
	$C5H5^{PA}\cdots O^{W}$	0.00621	0.02321	0.00085	-0.00411	0.00496
	$O1H6^{PA}\cdots O^{W}$	0.02542	0.11139	0.00309	-0.02166	0.02476
PW2	$C8H8^{PA}\cdots O2^{PA}$	0.01602	0.06367	0.00213	-0.01165	0.01379
	$C4H4^{PA}\cdots O^{W}$	0.00603	0.02148	0.00072	-0.00393	0.00465
	$NH9^{PA}\cdots O^{W}$	0.01826	0.08051	0.00318	-0.01377	0.01695
PW3	$C8H8^{PA}\cdots O^{W}$	0.00855	0.03728	0.00167	-0.00598	0.00765
	$OH1^{W}\cdots O2^{PA}$	0.02097	0.09923	0.00381	-0.01719	0.02100
PW4	$C8H8^{PA}\cdots O2^{PA}$	0.01419	0.05604	0.00188	-0.01024	0.01213
	$C7H7^{PA}\cdots O^{W}$	0.00764	0.02881	0.00109	-0.00503	0.00612
	$OH1^{W}\cdots O1^{PA}$	0.01970	0.08973	0.00345	-0.01554	0.01898
PW5	$OH1^{W}\cdots O2^{PA}$	0.01834	0.07905	0.00299	-0.01378	0.01677
PW6	$C8H8^{PA}\cdots O2^{PA}$	0.01293	0.05165	0.00174	-0.00943	0.01117
	$OH1^{W}\cdots O2^{PA}$	0.02609	0.11010	0.00276	-0.02200	0.02476
	$C1H1^{PA}\cdots O^{W}$	0.00662	0.02804	0.00122	-0.00458	0.00579
PA	$C8H8^{PA}\cdots O2^{PA}$	0.01379	0.05435	0.00182	-0.00994	0.01176

Table 4. The second–order perturbation energies $E(2)$ (in kcal·mol^{-1}) of the H–bonds in PA–H_2O complexes obtained by NBO analysis.

complex	H–bond	$E(2)^a$
PW1	$C5H5^{PA}\cdots O^{W}$	0.38(0.11)
	$O1H6^{PA}\cdots O^{W}$	0.07(11.30)
PW2	$C8H8^{PA}\cdots O2^{PA}$	0.51
	$C4H4^{PA}\cdots O^{W}$	0.44(0.14)
	$NH9^{PA}\cdots O^{W}$	0.05(7.17)
PW3	$C8H8^{PA}\cdots O^{W}$	0.06(0.39)
	$OH1^{W}\cdots O2^{PA}$	3.60(1.66)
PW4	$C7H7^{PA}\cdots O^{W}$	0.09(0.75)
	$OH1^{W}\cdots O1^{PA}$	4.05(0.48)
PW5	$OH1^{W}\cdots O2^{PA}$	1.39(1.93)
PW6	$OH1^{W}\cdots O2^{PA}$	2.58(7.59)
	$C1H1^{PA}\cdots O^{W}$	0.25

[a] The values not in parentheses refer to H–bond formation via the O sp hybrid; those in parentheses refer to H–bond formation via the O p hybrid. See discussion in the text.

The result of NBO analysis is listed in Table 4. The O atom involved as H–acceptor in PW2 ($C8H8^{PA}\cdots O2^{PA}$) and PW6 ($C1H1^{PA}\cdots O^{W}$) has one sp branch, respectively, while the O atom in other H–bonds has two branches: one has sp hybrid characteristics, and the other one has p hybrid characteristics; they corresponds to two $E(2)$ values, respectively. Due to the largest $E(2)$ value of 11.37 kcal·mol^{-1}, the strongest CT effect happened in the $O1H6^{PA}\cdots O^{W}$ H–bond of PW1 and made contribution to the hydrogen bonding interaction to a great extent. Moreover, the intermolecular $OH1^{W}\cdots O2^{PA}$ (PW6) have larger $E(2)$ values (10.17 kcal·mol^{-1}), so CT effect plays an important role in it. The $E(2)$ values of H–bonds involving the methylene as H–donor are less than 1.0 kcal·mol^{-1} and are much smaller than those of the other H–bonds, which indicates that these H–bonds are very weak and is consistent with discussion above. It is pity that no direct NBO evidence for the $C8H8^{PA}\cdots O2^{PA}$ H–bond in some PA–H_2O complexes (PW1, PW4 and PW6) was found, one reasonable explanation is that it is too weak in these complexes, and another possible reason is that the natural bond orbital is basically localization so that NBO cannot treat with such delocalization H–bond, which have been discussed in our previous works [47].

The results of LMO-EDA are listed in Table 5. As shown in Table 5, the total interaction energy (ΔE_{MP2}) between PA and H_2O moieties is whithin the range of about -3.8 ~ -6.3 kcal×mol^{-1}, and the strongest ΔE_{MP2} of -6.29 kcal·mol^{-1} indicates that PW6 is the most stable PA–H_2O complex. In PW6, the largest stabilizing force is the exchange energy (ΔE_{ex}) of -13.44 kcal·mol^{-1}, which origins from the overlap between the spin orbital of each monomer and the like–spin orbitals of the other monomer, but coming with a strong repulsion energy (ΔE_{rep}) of 24.05 kcal×mol^{-1} simultaneously. The second largest stabilizing force is the electrostatic interaction (ΔE_{ele}) of -12.77 kcal·mol^{-1}. Moreover, the formation of the H–bond changes their orbital shapes of fragments and results in a polarization energy (ΔE_{pol}) of -3.74 kcal·mol^{-1}, which makes important contribution to the total interaction energy in PW6. In addition, the minor contribution to ΔE_{MP2} is the dispersion energy (ΔE_{disp}) of -0.39 kcal·mol^{-1}. In PW1, the second stable complex,

Table 5. The LMO–EDA results of PA–H_2O complexes obtained at the MP2 level. Energy values are given in kcal·mol^{-1}.

complex	PW1	PW2	PW3	PW4	PW5	PW6
ΔE_{ele}	-11.35	-9.03	-7.93	-9.64	-10.78	-12.77
ΔE_{ex}	-11.75	-9.22	-9.49	-11.06	-11.51	-13.44
ΔE_{rep}	21.21	16.04	16.83	19.13	20.23	24.05
ΔE_{pol}	-3.36	-2.20	-2.17	-2.52	-3.09	-3.74
ΔE_{disp}	-0.90	-0.95	-1.00	-1.57	-0.88	-0.39
ΔE_{MP2}	-6.16	-5.35	-3.76	-5.66	-6.02	-6.29
ΔE_{prep}	0.11	0.17	0.51	0.15	0.45	0.22

the main contributions to the second largest ΔE_{MP2} (-6.16 kcal·mol^{-1}) mainly come from the larger ΔE_{ele} (-11.35 kcal·mol^{-1}) and ΔE_{ex} (-11.75 kcal·mol^{-1}), while ΔE_{pol} (-3.36 kcal·mol^{-1}) and ΔE_{disp} (-0.90 kcal·mol^{-1}) make less contribution to the ΔE_{MP2} of PW1. Similar things also happened in PW2, PW4 and PW5 since they have almost same stabilities with each other. PW3 is the complex with less stabilities due to the smaller ΔE_{MP2} (-3.76 kcal·mol^{-1}), which is attributed to the weaker hydrogen bonding interactions in it.

Our previous studies showed that hydrogen bonding interaction is not the unique factor for the stability of complexes involving hydrogen bonding interactions [51-55]. Therefore, the influence of the deformation of the monomers on the stability of PW complex were taken into account. On the basis of NBO theory, the preparation energy (ΔE_{prep}) is the amount of energy required to deform the separate bases from their free monomer structure to the geometry that they acquire in the pair complex,

$$\Delta E_{prep} = E_{PW} - E_{PA(W)} - E_{W(PA)} \qquad (1)$$

here $E_{PA(W)}$ (or $E_{W(PA)}$) is the energy of the PA (or water) monomer when all the nucleus structure units of water (or PA) are considered as puppet atoms of carrying empty orbital. ΔE_{prep} is positive because the structural deformation causes the molecular energy to jump to a higher energy level, while ΔE_{MP2} is negative unless the complex is less stable than the monomers. The preparation energies of all PA–H_2O complexes are also listed in Table 5. All complexes have small ΔE_{prep} values of less than about 0.7 kcal·mol^{-1}. The two largest ΔE_{prep} values are 0.51 (PW3) and 0.45 (PW5) kcal×mol^{-1}, which indicates that the cleavages of the intramolecular $C8H8^{PA}\cdots O2^{PA}$ H–bond in PW3 and PW5 result in the serious structural deformation and counteracts such strong hydrogen bonding interactions to a great extent. On the contrary, the intramolecular $C8H8^{PA}\cdots O2^{PA}$ H–bond was retained in other PA–H_2O complexes (PW1, PW2, PW4 and PW6), and the structural deformation of them are slight, which can be learned from their smaller ΔE_{prep} values in Table 5. In one word, both hydrogen bonding interaction and structural deformation are the two important aspects of the stability of PA–H_2O complexes, which is consistent with our previous works [51-55].

4. CONCLUSIONS

The geometries, energies and IR characteristics of the H–bonds of PA–H_2O complexes were studied at the MP2/6–311++G(d,p) level. The intramolecular $C8H8^{PA}\cdots O2^{PA}$ H–bond is retained in all complexes except PW3 and PW5. The intermolecular $O1H6^{PA}\cdots O^{W}$ (PW1) and $OH1^{W}\cdots O2^{PA}$ (PW6) H–bonds are the two strongest ones. The H–bonds involving the methylene of PA as H–donors are very weak. Both hydrogen bonding interaction and structural deformation play important roles in the relative stabilities of the complexes. Except PW3, all PA–H_2O complexes have similar stabilities, which indicates that PA inclines to form various complexes when it meets with water solvent. These results further reinforce the concept that PA is considered as a good electron acceptor (or donor) in forming complexes with various small organic molecules. Therefore, we think that the studies on PA-H_2O complexes maybe bear significance to the understanding the hydrogen bonding interactions between PA and other small organic molecules.

ACKNOWLEDGEMENT

This work is supported by the Natural Science Foundation of Tianjin (No. 12JCYBJC13400) and the Program for Innovative Research Team in University of Tianjin (TD13-5074).

REFERENCES

1. M. Sciskalska, M. Sliwinska-Mosson, M. Podawacz, W. Sajewicz and H. Milnerowicz, *Drug. Chem. Toxicol.* **38**, 121 (2015).
2. W.S. Waring, H. Jamie and G.E. Leggett, *Hum. Exp. Toxicol.* **29**, 63 (2010).
3. M. Naggayi, N. Mukiibi and E. Iliya, *Afr. Health. Sci.* **15**, 598 (2015).
4. S.B.K. Mahadevan, P.J. McKiernan, P. Davies and D.A. Kelly, *Arch. Dis. Child.* **91**, 598 (2006).
5. M. Cekmen, Y.O. Ilbey, E. Ozbek, A. Simsek, A. Somay and C. Ersoz, *Food Chem. Toxicol.* **47**, 1480 (2009).
6. P. Abraham, *Nephrology.* **10**, 623 (2005).
7. N.V. Nayyer, J. Byers and C. Marney, *Brit. Dent. J.* **216**, 229 (2014).
8. P. Marzuillo, S. Guarino and E. Barbi, *Eur. J. Pediatr.* **173**, 415 (2014).
9. A.-R. Marzilawati, Y.-Y. Ngau and S. Mahadeva, *BMC Pharmacol. Toxico.* **13**, 8 (2012).
10. H. Jaeschke, *Digest. Dis.* **33**, 464 (2015).
11. E.W. Holt, S. DeMartini and T.J. Davern, *J. Clin. Gastroenterol.* **49**, 790 (2015).
12. G.G. Graham, M.J. Davies, R.O. Day, A. Mohamudally and K.F. Scott, *Inflammopharmacology.* **21**, 201 (2013).
13. M.L. Ramos, J.F. Tyson and D.J. Curran, *Anal. Proc. incl. Anal. Comm.* **32**, 175 (1995).
14. P.A. Mosier-Boss, S.H. Lieberman and R. Newbery, *Appl. Spectrosc.* **49**, 630 (1995).
15. B.B. Ivanova, *J. Mol. Struct.* **738**, 233 (2005).
16. I.G. Binev, P. Vassileva-Boyadjieva and Y.I. Binev, *J. Mol. Struct.* **447**, 235 (1998).
17. E. Dreassi, G. Ceramelli, P. Corti, M. Massacesi and P.L. Perruccio, *Analyst.* **120**, 2361 (1995).
18. J.M. Beames and A.J. Hudson, *Phys. Chem. Chem. Phys.* **12**, 4157 (2010).
19. Y. Danten, T. Tassaing and M. Besnard, *J. Phys. Chem. A.* **110**, 8986 (2006).
20. S.J. Lee, A. Min, Y. Kim, A. Ahn, J. Chang, S.H. Lee, M.Y. Choi and S.K. Kim, *Phys. Chem. Chem. Phys.* **13**, 16537 (2011).
21. M. Yoosefian and N. Etminan, *RSC Adv.* **5**, 31172 (2015).
22. S. Rai, H. Singh and U.D. Priyakumar, *RSC Adv.* **5**, 49408 (2015).
23. K.H. Moller, A.S. Hansen and H.G. Kjaergaard, *J. Phys. Chem. A.* **119**, 10988 (2015).
24. M. Izadyar, M. Khavani and M.R. Housaindokht, *Phys. Chem. Chem. Phys.* **17**, 11382 (2015).
25. Z.G. Huang, Y.M. Dai and L. Yu, *Struct. Chem.* **21**, 863 (2010).
26. L.F. Guo, Z.G. Huang, T.T. Shen, L.L. Ma and X.Q. Niu, *Chin. J. Chem.* **31**, 1079 (2013).
27. P.L.A. Popelier: Atoms in Molecules: An Introduction (Prentice Hall, City, 2000).
28. C.F. Matta and R.J. Boyd: The Quantum Theory of Atoms in Molecules: From Solid State to DNA and Drug Design (WILEY-VCH Verlag GmbH & Co. KGaA, City, 2007).
29. A.E. Reed, L.A. Curtiss and F. Weinhold, *Chem. Rev.* **88**, 899 (1988).
30. P.F. Su and H. Li, *J. Chem. Phys.* **131**, 014102 (2009).
31. J. Xi and X. Xu, *Phys. Chem. Chem. Phys.* **18**, 6913 (2016).
32. S.K. Singh, S. Kumar and A. Das, *Phys. Chem. Chem. Phys.* **16**, 8819 (2014).
33. J.J. Panek, A. Filarowski and A. Jezierska-Mazzarello, *J. Chem. Phys.* **139**, 154312 (10 pp.) (2013).
34. A. Lakshmipriya, S.R. Chaudhari, A. Shahi, E. Arunan and N. Suryaprakash, *Phys. Chem. Chem. Phys.* **17**, 7528 (2015).

35. M. Jablonski and M. Palusiak, *J. Phys. Chem. A.* **116**, 2322 (2012).
36. L.L. Ma, Z.G. Huang, X.Q. Niu, T.T. Shen and L.F. Guo, *Comput. & Theor. Chem.* **1017**, 14 (2013).
37. E. Espinosa, I. Alkorta, J. Elguero and E. Molins, *J. Chem. Phys.* **117**, 5529 (2002).
38. U. Koch and P.L.A. Popelier, *J. Phys. Chem.* **99**, 9747 (1995).
39. W.D. Arnold and E. Oldfield, *J. Am. Chem. Soc.* **122**, 12835 (2000).
40. S. Jenkins and I. Morrison, *Chem. Phys. Lett.* **317**, 97 (2000).
41. S.J. Grabowski, W.A. Sokalski and J. Leszczynski, *J. Phys. Chem. A.* **110**, 4772 (2006).
42. L.F. Pacios, *J. Phys. Chem. A.* **108**, 1177 (2004).
43. A.E. Reed, F. Weinhold, L.A. Curtiss and D.J. Pochatko, *J. Chem. Phys.* **84**, 5687 (1986).
44. M.J. Frisch, G.W. Trucks, H.B. Schlegel, G.E. Scuseria, M.A. Robb, J.R. Cheeseman, G. Scalmani, V. Barone, B. Mennucci, G.A. Petersson, H. Nakatsuji, M. Caricato, X. Li, H.P. Hratchian, A.F. Izmaylov, J. Bloino, G. Zheng, J.L. Sonnenberg, M. Hada, M. Ehara, K. Toyota, R. Fukuda, J. Hasegawa, M. Ishida, T. Nakajima, Y. Honda, O. Kitao, H. Nakai, T. Vreven, J.A. Montgomery Jr., J.E. Peralta, F. Ogliaro, M. Bearpark, J.J. Heyd, E. Brothers, K.N. Kudin, V.N. Staroverov, R. Kobayashi, J. Normand, K. Raghavachari, A. Rendell, J.C. Burant, S.S. Iyengar, J. Tomasi, M. Cossi, N. Rega, J.M. Millam, M. Klene, J.E. Knox, J.B. Cross, V. Bakken, C. Adamo, J. Jaramillo, R. Gomperts, R.E. Stratmann, O. Yazyev, A.J. Austin, R. Cammi, C. Pomelli, J.W. Ochterski, R.L. Martin, K. Morokuma, V.G. Zakrzewski, G.A. Voth, P. Salvador, J.J. Dannenberg, S. Dapprich, A.D. Daniels, Ö. Farkas, J.B. Foresman, J.V. Ortiz, J. Cioslowski and D.J. Fox: Gaussian09, (Gaussian, Inc., City, 2009).
45. F. Biegler-König and J. Schönbohm: AIM2000, (University of Applied Sciences, City, 2000).
46. M.W. Schmidt, K.K. Baldridge, J.A. Boatz, S.T. Elbert, M.S. Gordon, J.H. Jensen, S. Koseki, N. Matsunaga, K.A. Nguyen, S. Su, T.L. Windus, M. Dupuis and J.A. Montgomery, *J. Comput. Chem.* **14**, 1347 (1993).
47. H.K. Wang, Z.G. Huang, T.T. Shen and L.F. Guo, *Struct. Chem.* **23**, 1163 (2012).
48. H.K. Wang, Z.G. Huang, T.T. Shen and L.F. Guo, *J. Mol. Model.* **18**, 3113 (2012).
49. L. Yu, Y.H. Wang, Z.G. Huang, H.K. Wang and Y.M. Dai, *Int. J. Quantum Chem.* **112**, 1514 (2012).
50. X.Q. Niu, Z.G. Huang, L.L. Ma, T.T. Shen and L.F. Guo, *J. Chem. Sci.* **125**, 949 (2013).
51. Z.G. Huang, L. Yu, Y.M. Dai and H.K. Wang, *Struct. Chem.* **22**, 57 (2011).
52. Z.G. Huang, L. Yu and Y.M. Dai, *Int. J. Quantum Chem.* **111**, 3915 (2011).
53. Z.G. Huang, Y.M. Dai, L. Yu and H.K. Wang, *J. Mol. Model.* **17**, 2609 (2011).
54. Z.G. Huang, L. Yu, Y.M. Dai and H.K. Wang, *J. Mol. Struct. (Theochem).* **960**, 98 (2010).
55. Z.G. Huang, L. Yu and Y.M. Dai, *Struct. Chem.* **21**, 855 (2010).